Plant Ecology and Evolution 158 (2): 205–213, 2025
https://doi.org/10.5091/plecevo.140133

RESEARCH ARTICLE

Calcium oxalate crystals in leaves of *Randia* (Gardenieae, Rubiaceae): environmental response or diagnostic character?

Mayte Stefany Jiménez-Noriega[1], Alejandro De la Rosa-Tilapa[1], Alejandro Torres-Montúfar[2]

1 Jardín Botánico FES-Cuautitlán, Departamento de Ciencias Biológicas, Facultad de Estudios Superiores Cuautitlán, Universidad Nacional Autónoma de México (FESC-UNAM), México

2 Herbario FES-Cuautitlán, Departamento de Ciencias Biológicas, Facultad de Estudios Superiores Cuautitlán, Universidad Nacional Autónoma de México (FESC-UNAM), México

Corresponding author: Mayte Stefany Jiménez-Noriega (mayte.jimenez@cuautitlan.unam.mx)

Academic editor: Elmar Robbrecht ♦ **Received** 24 October 2024 ♦ **Accepted** 13 March 2025 ♦ **Published** 4 June 2025

Abstract

Background and aims – Calcium oxalate crystals are the most common biominerals in plants and have a wide variety of forms, such as styloids, druses, raphides, prisms, and crystal sand. The shape, position, and number of crystals in plant tissues can have taxonomic value. For Rubiaceae, one of the most diverse angiosperm families, the presence of crystals may be taxonomically informative. In Mexico, one of the most diverse Rubiaceae genera is *Randia*, which occurs in arid, tropical, temperate, and coastal dune vegetation. The aim of this study is to explore the taxonomic value of calcium oxalate crystals in *Randia*. Furthermore, we aim to ascertain whether these crystals respond to the environmental conditions in which the plant grows.

Material and methods – Ten Mexican *Randia* species were selected, three of which included individuals from different vegetation types. For each individual, three mature leaves obtained from herbarium samples from MEXU and FESC were selected for SEM processing and leaf clearing.

Key results – Druses in the spongy parenchyma and palisade parenchyma were constant in all the species studied. The druses in the palisade parenchyma were always larger than those in the spongy parenchyma. In addition to druses in the intracellular parenchyma, *R. tomatillo* presented extracellular prisms in the epidermis as well as extracellular prisms and aggregate prisms in the mesophyll, which is a rare characteristic in Rubiaceae.

Conclusion – The constant presence of druses in the mesophyll could serve as a possible characteristic to diagnose the genus *Randia*, whereas the variable presence of druse crystals in the epidermis and veins could be related to environmental factors. The prisms in *R. tomatillo* may be related to its occurrence in the harsh environment of coastal dunes.

Keywords

druses, extracellular prisms, leaves, *Randia*, palisade parenchyma, spongy parenchyma

INTRODUCTION

In plants, three typical forms of biominerals occur: calcium carbonate, amorphous silica, and calcium oxalate (Franceschi and Horner 1980; Arnott 1982; Franceschi and Nakata 2005; Bauer et al. 2011); the last is the most common (McNair 1932; Franceschi and Nakata 2005). Raphides, styloids, druses, prisms, and crystal sand are part of the great morphological diversity of calcium oxalate crystals (Franceschi and Nakata 2005; Raman et al. 2014). The shape, type, and number of these crystals, as well as their location in the plant body, have taxonomic significance (Franceschi and Horner 1980; Prychid and Rudall 1999; Hartl et al. 2003; Prychid et al. 2003; Leszczuk et al. 2014). Crystal formation can be a product of genes (Franceschi and Nakata 2005; Kausch and Horner 1982),

Plant Ecology and Evolution is published by Meise Botanic Garden and the Royal Botanical Society of Belgium.

the environment (Faheed et al. 2013), or a combination of both (Franceschi and Nakata 2005).

Calcium oxalate crystals have been identified in approximately 215 plant families, including Rubiaceae (McNair 1932), which is the fourth-largest flowering plant family with more than 14,000 species (Razafimandimbison and Rydin 2024). For Rubiaceae, the systematic value of crystals has been evaluated at different taxonomic levels; for example, the presence of raphides is diagnostic for the Rubioideae subfamily in some classification schemes (Verdcourt 1958; Bremekamp 1966), at the generic level, as in members of the tribe Chiococceae (Aiello 1979), and at the species level, e.g. *Simira* Aubl. (Moraes et al. 2009) or *Cephalanthus* L. (Romero et al. 2019).

In Mexico, Rubiaceae is one of the most diverse plant families, with 111 genera and 724 species, among which *Randia* L. stands out as the second most diverse genus, with 64 species (Torres-Montúfar and Torres-Díaz 2022). It comprises trees, shrubs, and lianas. It occurs in arid regions and grows in deciduous and evergreen vegetation from sea level to 3300 m in elevation (Borhidi 2012). The neotropical genus *Randia* is a member of the tribe Gardenieae and comprises approximately 90 species (Gustafsson 1998, 2000; Gustafsson and Persson 2002; Judkevich et al. 2020). The morphology of the genus is diverse with respect to habit (trees, shrubs, and lianas), leaf shape, and floral sexuality (mainly dioecious, but with some bisexual species). It is characterized by the presence of brachyblasts bearing clustered stipules and leaves, pollen grains released in tetrads, and fleshy fruits containing numerous discoidal seeds embedded in dark pulp (Gustafsson 2000; Borhidi 2019; Lorence 2012; Judkevich et al. 2015, 2016, 2020). *Randia* is considered a taxonomically problematic group (Borges et al. 2021). The aim of our study is to identify crystal types in *Randia* and explore their locations in leaf tissue as well as their associations with different vegetation types.

MATERIAL AND METHODS

This study was conducted on 10 taxa of *Randia* from different vegetation types. For some species, several samples from different vegetation types were collected. Three mature leaves per individual were removed from herbarium samples deposited at FESC and MEXU (acronyms follow Thiers 2025). A list of the species studied and voucher information is given in Table 1.

Scanning electron microscopy

Parts of the leaf blade (1 × 1 cm) were cut from the leaf samples, and hand-made transverse sections were obtained. The samples were dehydrated in a graded ethanol series (50–100%), incubated for 24 h at each concentration, and critical point dried with carbon dioxide. The samples were mounted on a metal stub with carbon adhesive tabs, gold coated, and examined at 15 kV with a Hitachi Stereoscan Model SU1510 SEM (Hitachi Ltd., Tokyo, Japan) at the Laboratorio de Microscopia y Fotografia de la Biodiversidad, Instituto de Biologia, Universidad Nacional Autonoma de Mexico.

Paraffin embedding

Portions of the middle region of the leaf, including the intercostal area from the midvein to the margin, were cut, rinsed, and dehydrated in increasing concentrations of tert-butanol (10–100%) for 24 h at each concentration. The tissues were embedded in paraffin (melting point 56°C), and transverse sections 10–18 µm in thickness were cut with an Ecoshel 315 rotatory microtome. The resulting sections were stained with safranin-fast green (Johansen 1940) and mounted with synthetic resin.

Leaf clearings

The procedure described by Lersten and Horner (2011) was followed. The samples were rehydrated for 24 h with 50% ethanol, followed by rinsing with deionized water. They were placed in a solution of commercial sodium hypochlorite (5% active chlorine) and water (1:1 ratio) until the pigments were gradually removed. Once the samples were bleached, they were rinsed with deionized water at least three times to remove any excess solution and subsequently dehydrated in a graded ethanol series (50–100%) with replacement every 30 minutes. Afterward, they were immersed in a mixture of absolute ethanol and xylene (1:1 ratio) and cleared with xylene. Once the leaf was cleared, it was mounted on a microscope slide with synthetic resin.

Image acquisition

Images were captured with a Primostar 3 microscope coupled with an Axiocam 208 colour camera and processed with ZEN lite software v.3.0 (Zeiss, Germany). Polarized light images were acquired via the two polarizing filters in the polarizing microscope: the polarizer and the analyser.

Crystal measurements

Crystal size measurements were conducted via ZEN lite software, with 30 diameter measurements taken per individual. The number of crystals per square millimetre (nc/mm^2) was calculated according to the methodology described by Altamirano et al. (2018), using a reference area of 0.2762 mm^2. Depending on the leaf size, five to ten areas per leaf were analysed. Crystal counting was performed manually with ImageJ software v.1.53t, employing the Multi-point Tool function (Schneider et al. 2012).

The crystal types and their locations in the tissue (epidermis (ep), palisade parenchyma (pp), spongy parenchyma (sp), and vascular bundle (vb)) were obtained from cross-sectional samples via SEM. Furthermore, hand sections were cleared, paraffin-embedded, and observed through a light microscope under polarized light. In addition, for the druse size in pp and sp, and for crystal

Table 1. Voucher information of the *Randia* species sampled.

Taxon	Voucher	Herbarium	Locality	Vegetation type
Randia aculeata L.	*H. Ochoterena 891* (*HO891*)	MEXU	Oaxaca	Cloud forest
Randia aculeata L.	*H. Ochoterena 639* (*HO639*)	MEXU	Veracruz	Dry forest
Randia capitata DC.	*A. Bonfil 275* (*AB275*)	FESC	Guerrero	Oak forest
Randia capitata DC.	*J. Calonico 21522* (*JC21522*)	MEXU	Campeche	Dry forest
Randia capitata DC.	*R. Medina 5703* (*RM5703*)	MEXU	Puebla	Xerophilous scrub
Randia echinocarpa Moc. & Sessé ex DC.	*A. Bonfil 4* (*AB4*)	FESC	Morelos	Dry forest
Randia hidalgensis Lorence	*M. Aguilar 9* (*MA9*)	MEXU	Hidalgo	Dry forest
Randia laetevirens Standl.	*H. Ochoterena 679* (*HO679*)	MEXU	Oaxaca	Cloud forest
Randia laetevirens Standl.	*M. Aguilar 53* (*MA53*)	MEXU	Hidalgo	Pine forest
Randia pterocarpa Lorence & Dwyer	*A. Torres-Montufar 816* (*ATM816*)	MEXU	Veracruz	Tropical rainforest
Randia retroflexa Lorence & M.Nee	*A. Torres-Montufar 940* (*ATM940*)	MEXU	Veracruz	Tropical rainforest
Randia thurberi S.Watson	*L. Albarran 7* (*LA7*)	FESC	Guerrero	Dry forest
Randia thurberi S.Watson	*F. Miranda 1940* (*FM1940*)	MEXU	Chiapas	Dry forest
Randia tomatillo Loes.	*L. Gonzalez-Quintero 4534* (*LQ4553*)	MEXU	Veracruz	Coastal dunes
Randia xalapensis M.Martens & Galeotti	*J.I. Calzada 11866* (*JIC11866*)	MEXU	Veracruz	Tropical rainforest
Randia xalapensis M.Martens & Galeotti	*A. Torres-Montufar 664* (*ATM664*)	MEXU	Veracruz	Tropical rainforest

abundance, observations were made in extended leaf blades that were cleared. Only the middle part of the leaf was quantified. By measuring the diameter of 30 crystals/individual/species, the number of crystals per square millimetre was quantified considering a reference area of 0.2762 mm^2 and, subsequently, the number of crystals per mm^2 observed in leaf surface.

RESULTS

The results detailed below are summarized in Table 2.

Crystal types and distribution

All the sampled species of *Randia* had intracellular druse crystals in the leaf mesophyll, notably in the spongy parenchyma and palisade parenchyma (Fig. 1A, E). *Randia tomatillo* also presented solitary bipyramidal prisms extracellularly (over or across the cell wall) and aggregated bipyramidal prisms in the epidermis and mesophyll (Fig. 1B–D). The size of these solitary bipyramidal prisms was 5 to 10 μm.

Druses in the epidermis

Druses were observed only in the epidermis of the *R. capitata* sample growing in the dry forest. The other species did not have druses in the epidermis, nor were they present in the two other samples of *R. capitata* growing in oak forest and xerophilous scrub.

Druses in the mesophyll

In all the samples studied for all vegetation types, druses were observed in the palisade and spongy parenchyma. In general, the druses present in palisade parenchyma were larger than those present in spongy parenchyma. In the spongy parenchyma, druses were scarce and varied in size among individuals from different localities and vegetation types (Fig. 2C–E).

Druses in the midvein

Druses were observed in the parenchyma of the central vascular bundle in *R. hidalgensis* (dry forest; Fig. 2A) and in one of the samples of *R. thurberi* (dry forest, *LA7*). In samples from different vegetation types, druses were present in the parenchyma of the central vascular bundle in *R. aculeata* (cloud forest, *HO891*), *R. retroflexa* (tropical rainforest), and *R. capitata* (xerophilous scrub, *RM5703*; Fig. 2B), whereas the rest of the samples of other vegetation types of these three species did not present druses in the central vascular bundle.

Crystal size

In general, the druses in the palisade parenchyma were larger than those in the spongy parenchyma (Fig. 2C–E). The largest druses in the palisade parenchyma were found in *R. capitata* from dry forest (30.62 ± 1.41), in two samples of *R. thurberi* from dry forest (*FM1940*: 31.11 ± 5.73, *LA7*: 29.42 ± 4.51 μm), and in *R. tomatillo* occurring in coastal dunes (27.77 ± 3.38 μm), while the rest of the values ranged from 7.35 μm to 14.52 μm. In the spongy parenchyma, the largest druses were found in one sample of *R. capitata* (24.8 ± 2.11 μm; Fig. 2C) and one sample of *R. thurberi* (20.61 ± 2.81 μm), both from dry forest. The smallest druses were found in one sample of *R. xalapensis* from rainforest *ATM664* (3.28 ± 0.35 μm; Fig. 2D), in one sample of *R. capitata* from oak forest (4.3 ± 0.4 μm), and in the single sample of *R. tomatillo* from coastal dunes

Table 2. Comparison of the calcium oxalate crystals in the leaves of Randia and vegetation type. ep = epidermis, pp = palisade parenchyma, sp = spongy parenchyma, vb = vascular bundle. (+) druses, (*) prisms, (-) druses absent. Mean and standard deviation.

Taxon	Vegetation type	ep	pp	sp	vb	Druse size in pp (µm)	Druse size in sp (µm)	Crystal abundance/ mm²
R. aculeata	Cloud forest (*HO891*)	-	+	+	+	10.18±1.23	9.15±1.28	1687.18
	Dry forest (*HO639*)	-	+	+	-	12.67±1.54	8.15±1.04	387.4
R. capitata	Dry forest (*JC21522*)	+	+	+	-	30.62±1.41	24.88±2.11	123.09
	Xerophilous scrub (*RM 5703*)	-	+	+	+	13.63±0.62	8.92±1.23	405.5
	Oak forest (*AB275*)	-	+	+	-	9.40±1.23	4.30±0.40	220.85
R. echinocarpa	Dry forest (*AB4*)	-	+	+	-	7.35±0.89	7.12±1.35	Not counted
R. hidalgensis	Dry forest (*MA9*)	-	+	+	+	13.9±1.15	13.82±1.57	1904.41
R. laetevirens	Pine forest (*MA53*)	-	+	+	-	14.52±1.16	10.53±1.70	485.15
	Cloud forest (*HO679*)	-	+	+	-	12.55±1.63	10.66±0.89	115.81
R. pterocarpa	Tropical rainforest (*ATM816*)	-	+	+	-	13.73±1.72	13.88±1.80	1614.77
R. retroflexa	Tropical rainforest (*ATM940*)	-	+	+	+	11.43±1.48	10.48±1.18	2107.16
R. thurberi	Dry forest (*FM1940*)	-	+	+	-	31.11±5.73	20.61±2.81	108.61
	Dry forest (*LA7*)	-	+	+	+	29.42±4.51	9.79±1.49	181.02
R. tomatillo	Coastal dunes (*LQ4553*)	*	+/*	+/*	-	27.77±3.38	4.98±1.03	640.83
R. xalapensis	Tropical rainforest (*ATM664*)	-	+	+	-	13.08±1.28	3.28±0.35	2143.37
	Tropical rainforest (*JIC11866*)	-	+	+	-	12.91±1.17	8.02±0.88	1017.37

(4.98 ± 1.03 µm), with the remaining values ranging from 7.12 µm to 13.9 µm.

The size of the druses in the spongy parenchyma ranged from 7.12 µm (*R. echinocarpa*) to 24.88 µm (*R. capitata*) in species from dry forest, from 9.15 µm (*R. aculeata*) to 10.66 µm (*R. laetevirens*) in cloud forest, and from 3.28 µm (*R. xalapensis*, *ATM664*) to 13.88 µm (*R. pterocarpa*) in rainforest. The druse size was 10.53 µm in the only species from pine forest (*R. laetevirens*), 8.92 µm in the species from xerophilous scrub (*R. capitata*), 4.3 µm in the species from oak forest (*R. capitata*), and 4.98 µm in the species from coastal dunes (*R. tomatillo*).

Crystal abundance

The highest number of druses per mm² was encountered in one of the two samples of *R. xalapensis ATM664* (2143.37 per mm²) and in the single sample of *R. retroflexa* (2107.16 per mm²), both from rainforest. High numbers were also encountered in the sample of *R. hidalgensis* (1904.41 per mm²) from dry forest and in *R. pterocarpa* (1614.77 per mm²) from rainforest, as well as in one of the three samples of *R. aculeata* (1687.18 per mm²) from cloud forest and the second sample of *R. xalapensis* from rainforest *JIC11866* (1017.37 per mm²). The lowest druse density was encountered in one sample of *R. thurberi* (108.61 per mm²) from dry forest *FM1940*. The crystal density could not be counted in *R. echinocarpa* due to the large number of trichomes.

The number of crystals was 485.15 per mm² for pine forest (based on a single sample), 115.81 per mm² for cloud forest in *R. laetevirens* and 1687 per mm² in *R. aculeata*. In species with samples from different types of vegetation, the crystal abundance was variable; for *R. capitata*, the sample with the highest crystal density was from xerophilous scrub (405.5 per mm²), followed by oak forest (220.85 per mm²) and dry forest (123.09 per mm²).

In *R. thurberi* (dry forest) samples from different localities but from the same type of vegetation, the number of druses ranged from 108.61 per mm² to 181.02 per mm², while in *R. xalapensis* (rainforest), it ranged from 1017.37 per mm² to 2143.37 per mm².

Surface distribution patterns

Three types of crystal distribution were recorded: (1) druses in the mesophyll but not in the midvein or the lateral veins (*R. thurberi*, *R. tomatillo*) (Fig. 3A), (2) druses in the mesophyll and lateral veins but absent in the midvein (*R. capitata*) (Fig. 3B), and (3) druses in the mesophyll, the midvein, and lateral veins (*R. hidalgensis*) (Fig. 3C).

DISCUSSION

Druses in *Randia* leaves have already been described in earlier general observations (Metcalfe and Chalk 1950). The presence of druses in the spongy parenchyma was consistent across all species of *Randia* studied here, regardless of the vegetation type from which the individuals were collected. This aligns with what has been reported by Martínez-Cabrera et al. (2009) for *R. aculeata* and *R. tetracantha* (Cav.) DC., and by Judkevich et al. (2015, 2020) for *R. brevituba* Judkevich & R.M.Salas and *R. heteromera* Judkevich & R.M.Salas from South America, where druses were observed in the same tissue. Given the significance of crystals at various taxonomic levels in Rubiaceae (e.g. Bremekamp 1966; Aiello 1979;

Moraes et al. 2009), this result could be a taxonomically important characteristic for the genus *Randia*, pending further studies in related genera.

All the species studied here and in other *Randia* species occurring in Argentina presented druses in the palisade parenchyma, except in *Randia micracantha* (Lillo) Bacigalupo (Judkevich et al. 2015). It should be noted, though, that we observed in this study that crystals were not maintained in leaf tissue embedded in paraffin or prepared for SEM observations. However, the crystals remain present in the cleared cross sections of the leaf blades. This phenomenon has been reported in the study

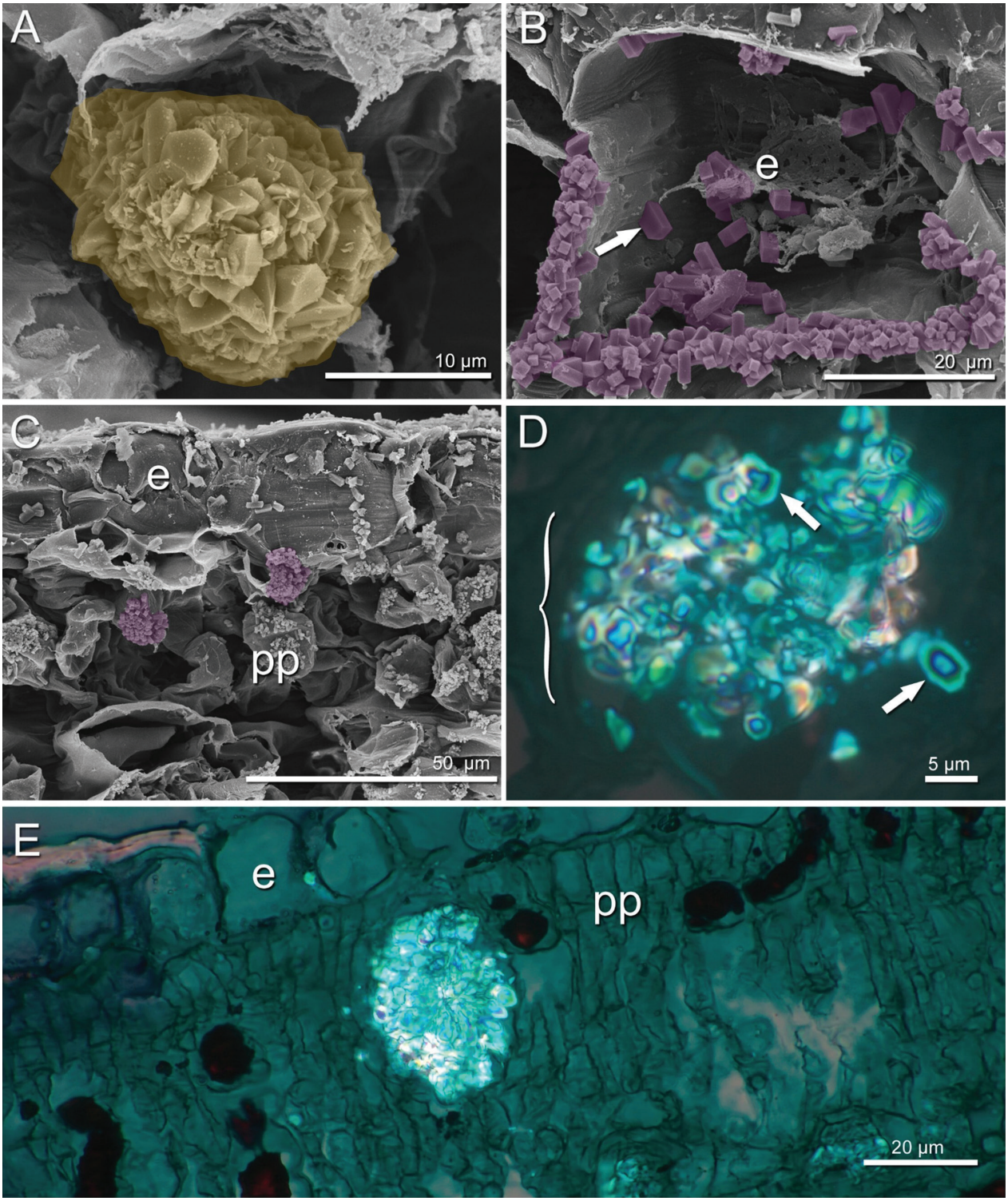

Figure 1. Presence of crystals in *Randia*. **A**. Intracellular druse in *Randia capitata* (artificially coloured in yellow, from *R. Medina 5703*, MEXU). **B**–**E**. *Randia tomatillo* (from *L. Gonzalez-Quintero 4534*, MEXU). **B**. Bipyramidal prisms (artificially coloured in purple) and extracellular prism (arrow). **C**. Prisms in the adaxial epidermis (artificially coloured in purple). **D**. Bipyramidal aggregate prisms (curly brackets) and bipyramidal prism (arrow). **E**. Druse in palisade parenchyma. e = epidermis, pp = palisade parenchyma.

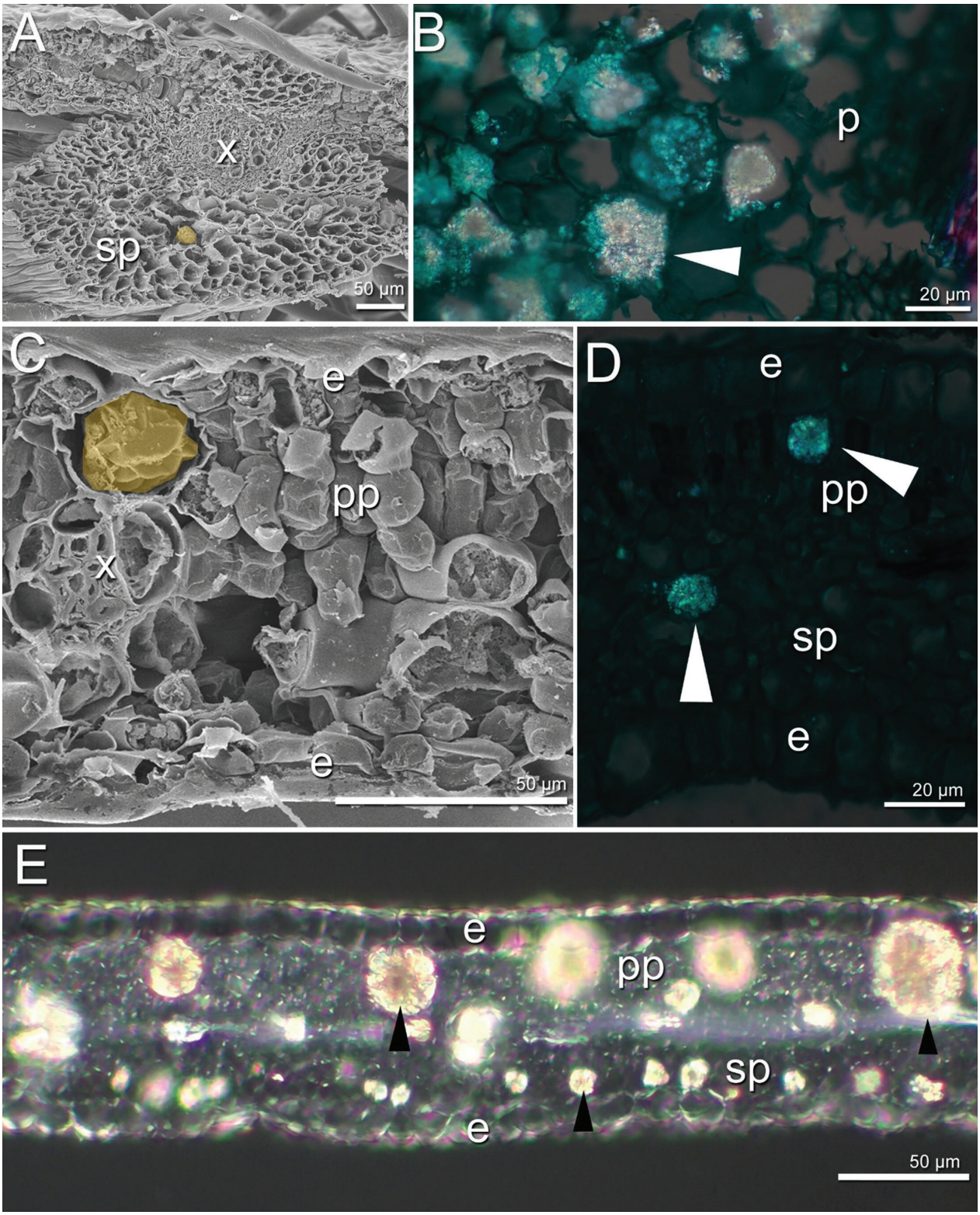

Figure 2. Crystals in the mesophyll and midveins of leaves. **A**. Druse in the midvein of *Randia hidalgensis* (artificially coloured in yellow, from *M. Aguilar 9*, MEXU). **B**. Druse in the midvein of *R. capitata* (arrow, from *R. Medina 5703*, MEXU). **C**. Druse in mesophyll of *R. capitata* (artificially coloured in yellow, from *A. Bonfil 275*, FESC). **D**. Druse in mesophyll of *R. xalapensis* (arrows, from *A. Torres-Montufar 664*, MEXU). **E**. Druses in mesophyll of *R. thurberi* (arrows, from *L. Albarran 7*, FESC). e = epidermis, p = parenchyma, pp = palisade parenchyma, sp = spongy parenchyma, x = xylem.

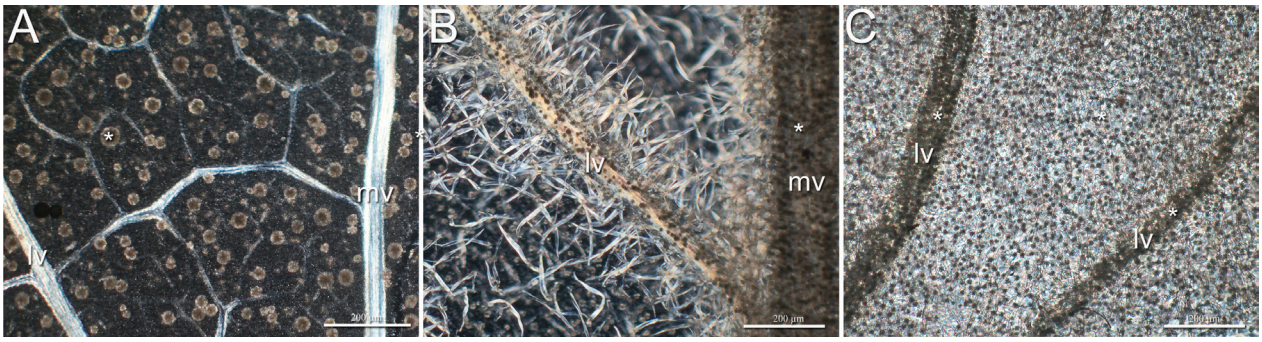

Figure 3. Crystal distribution patterns in leaves of *Randia*. **A**. Druses in the mesophyll in *R. thurberi* (from *L. Albarran 7*, FESC). **B**. Druses in the mesophyll and the lateral veins in *R. capitata* (from *R. Medina 5703*, MEXU). **C**. Druses in the mesophyll, the midvein, and the lateral veins in *R. hidalgensis* (from *M. Aguilar 9*, MEXU). mv = midvein, lv = lateral vein, * = druses. Scale bars = 200 μm.

by He and Kirilak (2014) in which the technique caused crystal dislodging or scattering.

Larger druses in the palisade parenchyma and smaller druses in the spongy parenchyma were also documented by Judkevich et al. (2015, 2020) in *Randia calycina* Cham., *Randia ferox* (Cham. & Schltdl.) DC., and *Randia heteromera*. Larger druses in photosynthetic parenchyma have been linked to light-reflective properties, which may help disperse light to surrounding chloroplasts (Kuo-Huang et al. 2007; Horner 2012). Additionally, they can channel light toward the parenchyma, enhancing photosynthetic efficiency (Pierantoni et al. 2017).

Druses in the epidermis (*R. capitata*) and vascular bundles (*R. aculeata*, *R. capitata*, *R. hidalgensis*, *R. retroflexa*, and *R. thurberi*) were not a consistent finding. They may or may not be present in individuals from the same type of vegetation but different localities (*R. thurberi* with druses in dry forest *LA7*, but not in dry forest *FM1940*). This difference could be due to calcium availability in the soil (Webb 1999; Faheed et al. 2013). The calcium that forms the crystals is obtained from the environment (Franceschi and Nakata 2005). The synthesis of oxalic acid and the formation of crystals takes place in the cell. Alternatively, the presence of druses may be a response to herbivory (Molano-Flores 2001).

The size of the crystals can vary depending on the type of cell in which they form and the amount of calcium available in the environment (Franceschi and Nakata 2005). In this study, no correlation was observed between the type of vegetation from which individuals originated and the size and number of crystals. However, in controlled greenhouse studies, a positive correlation was recorded between higher concentrations of calcium in the substrate and an increase in the number and size of crystals (Faheed et al. 2013).

Certain studies report a possible correlation between druse abundance and ambient conditions. For *Schinus terebinthifolia* Raddi (Anacardiaceae), De Souza et al. (2022) reported a higher number of druses in leaves of plants from restinga forest (a coastal ecosystem in Brazil) in contrast with leaves of plants growing in savannas. The only study that has performed a correlation analysis is that of Gómez-Espinoza et al. (2021); for *Colobanthus quitensis* (Kunth) Bartl. (Caryophyllaceae), they found that crystals in leaves were more abundant and larger in plants growing in mountainous environments with low temperatures and abundant rainfall than in plants inhabiting coastal areas. In contrast, some studies suggest the absence of a correlation between ambient conditions and crystals. Palchetti et al. (2014) observed the presence of leaf crystals in 13 species of *Capsicum* L. (Solanaceae) growing in both humid and dry regions of South America; only two species from humid regions lacked leaf crystals.

Extracellular prismatic crystals, a rare type of crystal among most angiosperms (Hartl et al. 2003, 2007), were observed in *R. tomatillo*. However, prior to this study, no records of extracellular crystals had been reported for Rubiaceae. These crystals may be present because *R. tomatillo* grows in coastal dunes. Due to high concentrations of windborne salt, wind speed, erosion, drought, salt spray, and nutrient scarcity (Alcaraz Ariza and Garre Belmonte 1985; Martínez and Moreno-Casasola 1996), plants that grow in these regions must exhibit physiological adaptations common to coastal halophytes, such as an increase in the size of water-storage tissues, cell wall elasticity, and a reduction in number of stomata (Alcaraz Ariza and Garre Belmonte 1985). Small crystals have been described in the epidermis of some species from various plant families distributed in coastal dunes; however, the presence of these crystals has not been associated with this type of vegetation and further studies are needed (Pérez-Cuadra and Cambi 2016).

CONCLUSION

This study highlights the importance and potential use of crystals in Rubiaceae taxonomy. The prismatic crystals observed in *R. tomatillo* have not previously been reported for Rubiaceae. The location and size of the druses is variable and, therefore, may be dependent on environmental factors such as the soil. This study can be a starting point for future research to investigate correlations of druses in *Randia*.

ACKNOWLEDGEMENTS

The authors thank Berenit Mendoza Garfias (IBUNAM) for her assistance with MEB photographs at IBUNAM. Special thanks to the herbarium curators and associate personal from MEXU and FESC. This research was supported by the Programa de Apoyo a Proyectos de Investigación e Innovación Tecnológica-UNAM: PAPIIT IA205224 and IA202622. We are grateful to the anonymous reviewers.

REFERENCES

Alcaraz Ariza F, Garre Belmonte M (1985) Las adaptaciones de las plantas en las dunas litorales del sureste de España. Anales de Biología 4: 11–14.

Altamirano SM, Borrelli N, Benvenuto ML, Honaine MF, Osterrieth M (2018) Calcium oxalate crystals in plant communities of the southeast of the Pampean Plain, Argentina. In: Endo K, Kogure T, Nagasawa H (Eds) Biomineralization. Springer, Singapore, 303–311. https://doi.org/10.1007/978-981-13-1002-7_32

Arnott HJ (1982) Three systems of biomineralization in plants with comments on the associated organic matrix. In: Nancollas GH (Ed.) Biological Mineralization and Demineralization. Dahlem Workshop Reports, vol. 23. Springer, Berlin and Heidelberg 199–218. https://doi.org/10.1007/978-3-642-68574-3_10

Aiello A (1979) A reexamination of *Portlandia* (Rubiaceae) and associated taxa. Journal of the Arnold Arboretum 60(1): 38–126. https://www.jstor.org/stable/43782518 [accessed 02.04.2025]

Bauer P, Elbaum R, Weiss IM (2011) Calcium and silicon mineralization in land plants: transport, structure and function. Plant Science 180(6): 746–756. https://doi.org/10.1016/j.plantsci.2011.01.019

Borhidi A (2012) Rubiáceas de México. Académiai Kiadó, Budapest, 1–608.

Borhidi A (2019) La Familia Rubiaceae en la Flora de México. Akadémiai Kiadó, Budapest, 1–704.

Borges RL, Razafimandimbison SG, Roque N, Rydin C (2021) Phylogeny of the Neotropical element of the *Randia* clade (Gardenieae, Rubiaceae, Gentianales). Plant Ecology and Evolution 154(3): 458–469. https://doi.org/10.5091/plecevo.2021.1889

Bremekamp CEB (1966) Remarks on the position, the delimitation and the subdivision of the Rubiaceae. Acta Botanica Neerlandica 15(1): 1–33. https://doi.org/10.1111/j.1438-8677.1966.tb00207.x

De Souza EV, Andrade GC, de Araújo HH, Dias-Pereira J (2022) Structural plasticity in leaves of *Schinus terebinthifolius* (Anacardiaceae) populations from three contrasting tropical ecosystems. The Journal of the Torrey Botanical Society 149(3): 187–193. https://doi.org/10.3159/torrey-d-22-00001.1

Faheed F, Mazen A, Elmohsen SA (2013) Physiological and ultrastructural studies on calcium oxalate crystal formation in some plants. Turkish Journal of Botany 37(1): 14. https://doi.org/10.3906/bot-1112-19

Franceschi VR, Horner HT (1980) Calcium oxalate crystals in plants. The Botanical Review 46: 361–427. https://doi.org/10.1007/BF02860532

Franceschi VR, Nakata PA (2005) Calcium oxalate in plants: formation and function. Annual Review of Plant Biology 56(1): 41–71. https://doi.org/10.1146/annurev.arplant.56.032604.144106

Gómez-Espinoza O, González-Ramírez D, Méndez-Gómez J, Guillén-Watson R, Medaglia-Mata A, Bravo LA (2021) Calcium oxalate crystals in leaves of the extremophile plant *Colobanthus quitensis* (Kunth) Bartl. (Caryophyllaceae). Plants 10(9): 1787. https://doi.org/10.3390/plants10091787

Gustafsson CGR (1998) The neotropical *Rosenbergiodendron*. Brittonia 50: 452–466. https://doi.org/10.2307/2807754

Gustafsson CGR (2000) Three new South American species of *Randia* (Rubiaceae, Gardenieae). Novon 10(3): 201–208. https://doi.org/10.2307/3393100

Gustafsson CGR, Persson C (2002) Phylogenetic relationships among species of the neotropical genus *Randia* inferred from molecular and morphological data. Taxon 51(4): 661–674. https://doi.org/10.2307/1555021

Hartl WP, Barbier B, Klapper HM, Barthlott W (2003) Dimorphism of calcium oxalate crystals in stem tissues of Rhipsalideae (Cactaceae) - a contribution to the systematics and taxonomy of the tribe. Botanische Jahrbücher für Systematik, Pflanzengeschichte und Pflanzengeographie 124: 287–302. https://doi.org/10.1127/0006-8152/2003/0124-0287

Hartl WP, Klapper H, Barbier B, Ensikat HJ, Dronskowski R, Müller P, Ostendorp G, Tye A, Bauer R, Barthlott W (2007) Diversity of calcium oxalate crystals in Cactaceae. Canadian Journal of Botany 85(5): 501–517. https://doi.org/10.1139/B07-046

He H, Kirilak Y (2014) Application of SEM and EDX in studying biomineralization in plant tissues. In: Kuo J (Ed.) Electron Microscopy. Methods in Molecular Biology, vol. 1117. Humana Press, Totowa, 663–675. https://doi.org/10.1007/978-1-62703-776-1_29

Horner HT (2012) *Peperomia* leaf cell wall interface between the multiple hypodermis and crystal-containing photosynthetic layer displays unusual pit fields. Annals of Botany 109(7): 1307–1316. https://doi.org/10.1093/aob/mcs074

Johansen DA (1940) Plant Microtechnique. MacGraw Hill, New York, 1–523.

Judkevich MD, Salas RM, Gonzalez AM (2015) Revisión de *Randia* (Rubiaceae) en Argentina, taxonomía y morfoanatomía. Boletín de la Sociedad Argentina de Botánica 50(4): 607–625. https://doi.org/10.31055/1851.2372.v50.n4.12920

Judkevich MD, Salas RM, Keller H (2016) *Randia brevituba* (Rubiaceae), a new species from the Southern Cone of America and comments on *Randia armata*. Systematic Botany 41(1): 238–244. https://doi.org/10.1600/036364416X690642

Judkevich MD, Gonzalez AM, Salas RM (2020) A new species of *Randia* (Rubiaceae) and the taxonomic significance of foliar anatomy in the species of *Randia* of the southern cone of America. Systematic Botany 45(3): 607–619. https://doi.org/10.1600/036364420X15935295449916

Kausch AP, Horner HT (1982) A comparison of calcium oxalate crystals isolated from callus cultures and their explant sources. Scan Electron Microscopy 1: 199–211.

Kuo-Huang L-L, Ku M, Franceschi V (2007) Correlations between calcium oxalate crystals and photosynthetic activities in palisade cells of shade-adapted *Peperomia glabella*. Botanical Studies 48(2): 155–164.

Lersten NR, Horner HT (2011) Unique calcium oxalate "duplex" and "concretion" idioblasts in leaves of tribe Naucleeae (Rubiaceae). American Journal of Botany 98(1): 1–11. https://doi.org/10.3732/ajb.1000247

Leszczuk A, Szczuka E, Stanisławek K, Mazurkiewcz I, Kasprzyk A (2014) Calcium oxalate crystals in the stem of *Sida hermaphrodita* (L.) Rusby (Malvaceae). Annales Universitatis Mariae Curie-Sklodowska, sectio C – Biologia 69(1): 41–48. https://doi.org/10.2478/umcsbio-2013-0003

Lorence DH (2012) *Randia*. In: Davidse G, Sousa MS, Knapp S, Chiang F (Eds) Flora Mesoamericana , Volume 4 (Part 2): Rubiaceae a Verbenaceae. Universidad Nacional Autónoma de México-Instituto de Biología, Missouri Botanical Garden, The Natural History Museum of London, St. Louis, USA, 241–253.

Martínez-Cabrera D, Terrazas T, Ochoterena H (2009) Foliar and petiole anatomy of tribe Hamelieae and other Rubiaceae. Annals of the Missouri Botanical Garden 96(1): 133–145. https://doi.org/10.3417/2006196

Martínez ML, Moreno-Casasola P (1996) Effects of burial by sand on seedling growth and survival in six tropical sand dune species from the Gulf of Mexico. Journal of Coastal Research 12: 406–419. https://www.jstor.org/stable/4298493 [accessed 16.04.2025]

McNair JB (1932) The interrelation between substances in plants: essential oils and resins, cyanogen and oxalate. American Journal of Botany 19(3): 255–272. https://doi.org/10.1002/j.1537-2197.1932.tb09649.x

Metcalfe CR, Chalk L (1950) Anatomy of the Dicotyledons: Leaves, Stem, and Wood in Relation to Taxonomy, with Notes on Economic Uses, vol. 2. Clarendon Press, Oxford, 725–1459.

Molano-Flores B (2001) Herbivory and calcium concentrations affect calcium oxalate crystal formation in leaves of *Sida* (Malvaceae). Annals of Botany 88(3): 387–391. https://doi.org/10.1006/anbo.2001.1492

Moraes TMS, Barros CF, Neto SJS, Gomes VM, Cunha M (2009) Leaf blade anatomy and ultrastructure of six *Simira* species (Rubiaceae) from the Atlantic Rain Forest, Brazil. Biocell 33(3): 155–165. https://doi.org/10.32604/biocell.2009.33.155

Palchetti MV, Barboza GE, Cosa MT (2014) Anatomía foliar en especies de *Capsicum* (Solanaceae) de diferentes ambientes biogeográficos sudamericanos. Boletín de la Sociedad Argentina de Botánica 49(3): 417–436. https://doi.org/10.31055/1851.2372.v49.n3.9473

Pérez-Cuadra V, Cambi V (2016) Caracteres epidérmicos de especies xero-halófilas: ¿es el ambiente el principal factor determinante? Lilloa 53(2): 282–298.

Pierantoni M, Tenne R, Brumfeld V, Kiss V, Oron D, Addadi L, Weiner S (2017) Plants and light manipulation: the integrated mineral system in okra leaves. Advanced Science 4(5): 1600416. https://doi.org/10.1002/advs.201600416

Prychid CJ, Rudall PJ (1999) Calcium oxalate crystals in monocotyledons: a review of their structure and systematics. Annals of Botany 84(6): 725–739. https://doi.org/10.1006/anbo.1999.0975

Prychid CJ, Rudall PJ, Gregory M (2003) Systematics and biology of silica bodies in monocotyledons. The Botanical Review 69(4): 377–440. https://doi.org/10.1663/0006-8101(2004)069[0377:SABOSB]2.0.CO;2

Raman V, Horner HT, Khan IA (2014) New and unusual forms of calcium oxalate raphide crystals in the plant kingdom. Journal of Plant Research 127(6): 721–730. https://doi.org/10.1007/s10265-014-0654-y

Razafimandimbison SG, Rydin C (2024) Phylogeny and classification of the coffee family (Rubiaceae, Gentianales): overview and outlook. Taxon 73(3): 673–717. https://doi.org/10.1002/tax.13167

Romero MF, Salas RM, Gonzalez AM (2019) Taxonomic and ecological implications of foliar morphoanatomy in *Cephalanthus* (Naucleeae, Rubiaceae). Systematic Botany 44(2): 378–397. https://doi.org/10.1600/036364419X15562052252207

Schneider CA, Rasband WS, Eliceiri KW (2012) NIH Image to ImageJ: 25 years of image analysis. Nature Methods 9: 671–675. https://doi.org/10.1038/nmeth.2089

Thiers B (2025) Index Herbariorum: a global directory of public herbaria and associated staff. New York Botanical Garden's Virtual Herbarium. https://sweetgum.nybg.org/science/ih/ [accessed 14.03.2025]

Torres-Montúfar A, Torres-Díaz AN (2022) Las Rubiáceas de México: ¿Ya está hecho el trabajo? Botanical Sciences 100(2): 446–468. https://doi.org/10.17129/botsci.2847

Verdcourt B (1958) Remarks on the classification of the Rubiaceae. Bulletin du Jardin botanique de l'État (Bruxelles) 28(3): 209–290. https://doi.org/10.2307/3667090

Webb MA (1999) Cell-mediated crystallization of calcium oxalate in plants. The Plant Cell 11(4): 751–761. https://doi.org/10.1105/tpc.11.4.751